NEOPLASIA
www.neoplasia.com

Volume 11 Number 10 October 2009 pp. 987–1002 **987**

Tumor-Endothelial Interaction Links the CD44$^+$/CD24$^-$ Phenotype with Poor Prognosis in Early-Stage Breast Cancer[1]

Martin Buess*,†, Michal Rajski†, Brigitte M.L. Vogel-Durrer†, Richard Herrmann†,‡ and Christoph Rochlitz†,‡

*Medical Oncology, St. Claraspital, Basel, Switzerland; †Department of Biomedicine, University of Basel, Basel, Switzerland; ‡Department of Medicine, Division of Oncology, University of Basel, Basel, Switzerland

Abstract

MATERIALS AND METHODS: The genomic effects of tumor-endothelial interactions in cancer are not yet well characterized. To study this interaction in breast cancer, we set up an *ex vivo* coculture model with human benign and malignant breast epithelial cells with endothelial cells to determine the associated gene expression changes using DNA microarrays. *RESULTS:* The most prominent response to coculture was the induction of the M-phase cell cycle genes in a subset of breast cancer cocultures that were absent in cocultures with normal breast epithelial cells. In monoculture, tumor cells that contained the stem cell–like CD44$^+$/CD24$^-$ signature had a lower expression of the M-phase cell cycle genes than the CD44$^-$/CD24$^+$ cells, and in the CD44$^+$/CD24$^-$ cocultures, these genes were induced. Pretreatment gene expression profiles of early-stage breast cancers allowed evaluating *in vitro* effects *in vivo*. The expression of the gene set derived from the coculture provided a basis for the segregation of the tumors into two groups. In a univariate analysis, early-stage tumors with high expression levels (n = 137) of the M-phase cell cycle genes had a significantly lower metastasis-free survival rate (P = 1.8e − 5, 50% at 10 years) and overall survival rate (P = 5e − 9, 52% at 10 years) than tumors with low expression (n = 158; metastasis-free survival, 73%; overall survival, 84%). *CONCLUSIONS:* Our results suggest that the interaction of endothelial cells with tumor cells that express the CD44$^+$/CD24$^-$ signature, which indicates a low proliferative potential, might explain the unexpected and paradoxical association of the CD44$^+$/CD24$^-$ signature with highly proliferative tumors that have an unfavorable prognosis.

Neoplasia (2009) 11, 987–1002

Introduction

Tumor angiogenesis is a prerequisite for tumor progression and metastasis. It is a complex process that requires cooperative reciprocal interaction of tumor cells and endothelial cells [1–4] and, thereby, offers an attractive therapeutic target [5]. Clinical trials with antiangiogenic agents, such as bevacizumab, which is an antibody against vascular endothelial growth factor (VEGF), introduced these agents into clinical practice [6]. During the last several years, antiangiogenic therapies, in combination with conventional chemotherapeutic agents, have been established for different tumor types, such as colorectal cancer [7], non–small cell lung cancer [8], renal cell cancer [9], and breast cancer [10]. The average clinical benefit of these drugs, however, is relatively modest, and it is unclear which patients benefit the most. Improvements are likely to come from a more thorough understanding of the molecular and cellular mechanisms that govern tumor-endothelial cell interactions. Tumor angiogenesis involves a plethora of soluble and cellular components that interact in a process of mutual signaling [11]. This requires a coordinated expression of proangiogenic factors [12] and suppression of antiangiogenic factors [13], which leads to endothelial cell proliferation and migration and vessel formation. Although multiple single genes have been described in numerous reports to be involved in angiogenesis, such as

Address all correspondence to: Martin Buess, St. Claraspital, Kleinriehenstrasse 20, CH-4016 Basel, Switzerland. E-mail: Martin.Buess@claraspital.ch

[1]This work was supported in part by the Swiss National Science Foundation grant 320000-112794/1 and a grant from Oncosuisse.
Received 21 April 2009; Revised 13 July 2009; Accepted 13 July 2009

DOI 10.1593/neo.09670

growth factors [12,14], membrane-bound molecules [15], and extracellular matrix components [16], there are likely others that have remained unidentified. The interplay between the various factors and their combined effects in tumor angiogenesis, however, remains to be further characterized.

Carcinomas are not merely aggregates of malignant epithelial cells but are, in many respects, organlike structures that include host stromal cells, such as fibroblasts, adipocytes, inflammatory cells, and the cells that form the tumor vasculature, and the malignant cells themselves that intermingle and interact with all of these cell types [17]. During the last few years, there has been growing evidence that, besides the cellular processes within the tumor cells, a relevant contribution to tumor progression is provided by the cells of the tumor microenvironment [18]. On the molecular level, genome-scale gene expression studies of many different carcinomas have illustrated in detail the complexity of the tumors and the diversity of the associated non–epithelial cell types [19]. Inductive interactions between these different cell types can play not only a morphogenetic role but also an important mechanistic role in the pathogenesis and progression of malignancy. The endothelial cells have so far been mainly viewed in the context of vessel formation to improve the blood supply of the tumor. However, relatively little is known about the paracrine effects of these tumor-endothelial cell interactions. It was commonly thought that the formation of new vessels would mainly be important for the transport of nutrients and oxygen to the tumor cells and that interrupting this support is the key mechanism of antiangiogenic therapies. If we assume that, by the interruption of the vascular support, the tumor gets more hypoxic, it seems paradoxical that antiangiogenic therapies enhance the effects of chemotherapy and radiation. In the hypoxic environment, these therapies have usually been shown to be less effective [20]. However, the effects of these agents could be due, in good part, to the disruption of the paracrine tumor-promoting signaling that occurs as a result of the interaction of the cancer and endothelial cells. Such reciprocal inductive signaling has been well known from developmental biology and has again attracted special attention with the concept of cancer stem cells and their stem cell niche [21]. Therefore, characterizing heterotypic cell-cell interaction effects on a global gene expression scale might help to better understand the currently used antiangiogenic agents and eventually lead to the identification of novel targets that could be used to interrupt these paracrine stimulatory signaling pathways. This study specifically focuses on the interaction between breast cancer cells and endothelial cells to identify their reciprocal signaling effects.

Breast cancer is a heterogeneous disease, which implies that the tumor-endothelial cell interactions might also be diverse. Tumor-endothelial cell interactions are not yet well characterized on a genome-wide scale, and they have not been compared between different tumor subtypes. Toward this aim, we performed a systematic analysis of the interactions between well-characterized breast cancer cell lines and primary endothelial cells in coculture.

We have recently used the approach of *in vitro* coculture experiments to characterize heterotypic interaction effects with DNA microarrays to systematically describe the global-scale effects that the tumor-fibroblastic stroma interaction has on gene expression. We identified a strong induction of an interferon response by specific tumor cells in coculture with a diverse set of fibroblasts, which corresponded to a subset of breast cancers with an unfavorable prognosis *in vivo* [22].

In this study, we used breast cancer cell lines and endothelial cells for systematic coculture experiments, which allowed the interaction effects to be characterized on a global gene expression scale. Using this system, we investigated the following hypotheses:

1. The interaction of tumor and endothelial cells leads to changes in gene expression, which are important for angiogenesis and tumor progression. The gene expression programs that are involved provide hints for the signaling mechanisms that are involved.
2. The interaction of tumor and endothelial cells leads to the induction of gene expression signatures that are clinically relevant. These interaction effects might account for a significant proportion of the unexplained information in the gene expression data from tissue specimens. Given the evidence that interactions between cells can play critical roles in tumor progression, these data might be even more meaningful than prominent expression patterns, which are driven by the proportional representation of a given cell type in a tissue.

We have performed a systematic overview of heterotypic interaction effects of breast cancer and endothelial cells. The picture we obtained is complex, but our results suggest that the interaction of endothelial cells with a subset of $CD44^+/CD24^-$ breast cancer cell lines induces a signature of "tumor-endothelial cell–induced M-phase cell cycle" genes, which is associated with a worse outcome in human breast cancer.

Materials and Methods

Cell Culture

Human mammary epithelial cells (HMECs; Cambrex Bio Science Walkersville, Walkersville, MD) were expanded in mammary epithelial basal medium that was supplemented with bovine pituitary extract, human epidermal growth factor, insulin, and antibiotics (Clonetics, Cambrex Bio Science Walkersville). MCF-7, T47D, MDA-MB-231, SKBR-3, Hs578T, and BT549 (ATCC, Atlanta, GA) were propagated in Dulbecco's modified Eagle medium that was supplemented with 10% FBS (HyClone, Logan, UT), glutamine, 100 U/ml penicillin, and 100 μg/ml streptomycin (Gibco, Grand Island, NY). Human umbilical vein endothelial cells (HUVECs; ATCC) and human dermal microvascular endothelial cells (HDMECs; Cambrex Bio Science Walkersville) were expanded in endothelial basal medium 2 (EBM2; Cambrex Bio Science Rockland, Rockland, ME) that was supplemented with human epidermal growth factor, hydrocortisone, GA-1000 (gentamicin, amphotericin-B), 5% FBS, VEGF, human fibroblast growth factor-B (with heparin), R3-IGF, and ascorbic acid. For the coculture experiments, the cells were cultivated for 48 hours at an equal density of 50,000 cells/cm^2 (25,000 tumor cells/cm^2 and 25,000 endothelial cells/cm^2) in endothelial basal medium (Cambrex Bio Science Rockland) supplemented with 0.2% FBS. This medium served as a good universal medium for all the cells in the study.

Proliferation Assays

Direct cell counting. For cell counting, prestarved cells were plated in quadruplicate in 24-well plates at a density of 50,000 cells/cm^2. After 24 and 48 hours, the cells were trypsinized and resuspended in 0.2 ml of FACS buffer that contained 0.5% BSA and 2 mM EDTA in PBS. The total cell number was determined using a cell counter.

WST-1 assay. The proliferation reagent 4-[3-(4-iodophenyl)-2-(4-nitro-phenyl)-2*H*-5-tetrazolio]-1,3-benzene disulfonate (WST-1; Roche

Diagnostics GmbH, Roche Applied Science, Mannheim, Germany) was used according to the manufacturer's instructions. WST-1 is changed by mitochondrial enzymes of metabolically active cells to a colorful formazan that can be measured at a wavelength of 450 nm. The cell number was determined by comparison of the absorbance values to a standard cell dilution curve.

Comparison of HUVECs Proliferation in Response to Different Conditioned Medium

To obtain the conditioned medium, 10e6, Hs578T, MDA-MB-231, MCF-7, or HUVECs were extensively washed to avoid transfer of any stimuli from the regular cell growth medium. The cells were kept in 10 ml of EBM2 that contained 0.2% FBS for 24 hours. The medium was then aspirated and filtered through a 0.2-nm pore filter. In parallel, 3000 HUVECs per well were plated in a 96-well plate and starved for 24 hours in EBM2 that contained 0.2% FBS. For the stimulation experiments, HUVECs were washed once with PBS and incubated for 48 hours in 1:2 diluted conditioned medium in EBM2 that contained 0.2% FBS. EBM2 that contained 0.2% FBS was used as a negative control (vehicle medium), HUVEC culture supernatant that was diluted 1:2 in vehicle medium was used as an autologous medium control, and the full endothelial cell growth medium 2 that contained 5% FBS and all the supplements that were described above was used as a positive control. To determine the cell growth in response to stimulation with conditioned medium, the cells were stained with 7% WST-1 in low-serum Dulbecco's modified Eagle medium (0.2% FBS) for 1 hour at 37°C in 5% CO_2. The absorbance was measured with an ELISA reader at a wavelength of 450 nm. Values for each experimental condition were obtained by calculating the average of at least eight independent replicates.

Inhibition with the Blocking Antibody Bevacizumab

To block the stimulatory effects of tumor cell conditioned media, the medium was supplemented with 100 ng/ml bevacizumab (Avastin; Genentech/Roche). To control the effect of bevacizumab, an additional HUVEC culture was set up with a medium that was enriched with recombinant VEGF-A (5 ng/ml) and 5% FBS. The cell growth was determined as above, and the absolute absorbance values were compared.

To check if blocking is specific for bevacizumab, trastuzumab (Herceptin; Genentech/Roche) was included at equal concentrations (0, 360, 720 ng/ml) in the analysis. As a negative control, HUVECs that were treated with Hs578T cell culture supernatant were used. The cell growth was determined as described before, and the absolute absorbance values were compared.

RNA Isolation and Amplification

After discarding the culture medium and washing the cell layer once with PBS, total RNA was isolated by lysing the cells in the culture dish with RLT buffer (Qiagen, Valencia, CA) and extracting with the RNeasy Mini Kit (Qiagen). Five hundred nanograms of total RNA was amplified using the Message Amp II aRNA Kit (Ambion, Austin, TX). The amplification product was checked for integrity by electrophoresis in a 1% agarose gel in MOPS buffer.

Complementary DNA Microarrays and Hybridization

The human complementary DNA (cDNA) microarrays contained 40,700 elements, which represented 24,472 unique genes that were based on Unique Clusters. The arrays were produced at the Stanford Functional Genomic Facility. Complete details regarding the clones on the arrays may be found at: http://www.microarray.org/sfgf/jsp/servicesFrame.jsp#productionArrays.

cDNA produced from 6 μg of amplified RNA were hybridized to the array in a two-color comparative format, with the experimental samples labeled with one fluorophore (Cy5) and a reference pool of messenger RNA (Universal Human Reference mRNA; Stratagene, La Jolla, CA) labeled with a second fluorophore (Cy3). The fluorescent dyes were purchased from Amersham Pharmacia Biotech (Piscataway, NJ). Hybridizations were carried out using the standard protocol that was described previously [19].

Data Analysis and Clustering

Array images were scanned using an Axon Scanner 4000B (Axon Instruments, Union City, CA), and image analysis was performed using GenePix Pro version 5.0 3.0.6.89 (Axon Instruments). The raw data files were stored in the Stanford Microarray Database [23], and the data that were used for the article are available at: http://microarray-pubs.stanford.edu/tumor-endothelial interaction. Data were expressed as the $\log_2$ ratio of fluorescence intensities of the sample and the reference for each element on the array.

The (Cy5/Cy3) ratio is defined in the Stanford Microarray Database [23] as the normalized ratio of the background-corrected intensities. Spots with aberrant measurements that were due to obvious array artifacts or poor technical quality were manually flagged and removed from further analysis. A filter was applied to omit measurements where the fluorescent signal from the DNA spot was less than 50% above the measured background fluorescence that surrounded the printed DNA spot in either the Cy3 or the Cy5 channel. Genes that did not meet these criteria for at least 80% of the measurements across the experimental samples were excluded from further analysis. Valid data were filtered to exclude elements that did not have at least a three-fold deviation from the mean in at least two samples. Data were evaluated by unsupervised hierarchical clustering [24] and significance analysis of microarray [25] and were displayed using TreeView (http://rana.lbl.gov/EisenSoftware.htm).

GO::Termfinder

GO::TermFinder comprises a set of object-oriented Perl modules for accessing Gene Ontology (GO) information and evaluating and visualizing the collective annotation of a list of genes to GO terms [26]. It can be used to draw conclusions from microarray and other biologic data by calculating the statistical significance of each annotation.

Determination of the Heterotypic Interaction Effect on Gene Expression

To facilitate the identification of heterotypic interaction effects on global gene expression in a mixed coculture experiment, the gene expression data were normalized based on the proportional contribution of each cell type to transcript abundance. Given that the average gene does not change because of the heterotypic interaction and that there are simple additive effects to account for, a linear regression fit was used for normalization. To determine the contribution of each cell type to the combined gene expression pattern in the linear regression model, the expression levels of the monocultures were the predictors, and the expression levels of the coculture were the response.

Specifically, a set of equations $(1 - n)$ was established (one per gene): $e_n^{\text{coculture}} = ((a \times e_n^{\text{monoculture1}}) + ((1 - a) \times e_n^{\text{monoculture2}})) \times I_n$, where e

represented the expression level of the gene, a represented the proportional contribution of mRNA from the respective monoculture, n represented the number of genes measured on the microarray, and I represented the interaction coefficient. We assume that the average gene is not influenced by the heterotypic interaction in the mixed coculture, which is represented as $I = 1$. Because the data set over e_{1_n} is skewed, a linear regression fit was empirically identified based on Gamma errors and identity link as a good model to calculate a. The equation $1 - n$ can then be solved for I_{1_n}, which results in a profile of interaction effects for the genes$_{1_n}$. These interaction effects can be analyzed in much the same way as conventional gene expression measurements.

Human Breast Cancer Data Set

The data set for breast cancer contained 295 tumors that were analyzed on a 25,000-spot oligonucleotide array [27]. In brief, patients were diagnosed and treated at the Netherlands Cancer Institute (NKI) for early-stage breast cancer (stages I and II) between 1984 and 1995. The clinical data were updated in January 2005. The median follow-up for patients who are still alive is 12.3 years.

The "tumor-endothelial cell–induced M-phase cell cycle" gene list consists of 98 genes that are represented by 95 image clones on the cDNA Stanford Array. Clones having the same Unigene locus were removed. The gene sequences were mapped to spots on the NKI array using Unigene build no. 184 (released on June 9, 2005) to give 36 unique spots. To overcome possible overweighting of clones from Unigene clusters that were matched to more than one probe on the NKI array, expression values that were derived from probes that were not matched to the same Unigene cluster were averaged. Expression measurements for each gene were mean centered. The resulting data set was subjected to hierarchical clustering with average linkage clustering [24] and displayed with TreeView (http://rana.lbl.gov/EisenSoftware.htm).

Distant metastasis was analyzed as first event only (distant metastasis-free probability). If a patient developed a local recurrence, an axillary recurrence, a contralateral breast cancer, or a second primary cancer (except for nonmelanoma skin cancer), he/she is censored at that time and the subsequent distant metastases are not analyzed. This is based on the theoretical possibility that the locally recurrent or second primary cancers could be a source for distant metastases. An ipsilateral supraclavicular recurrence was soon followed by a distant metastasis in all but one patient. An ipsilateral supraclavicular recurrence was thus considered to be the first clinical evidence for metastatic disease for this analysis, and patients were not censored at the time of ipsilateral supraclavicular recurrence. Overall survival was analyzed based on death from any cause, and patients were censored at last follow-up. Kaplan-Meier survival curves were compared by the Cox-Mantel log-rank test using Winstat for Microsoft Excel (R Fitch Software, Staufen, Germany).

A data set of gene expression patterns from advanced breast cancers was described by Sorlie et al. [28]. Expression data from 53 image clones that represented the "tumor-endothelial cell–induced M-phase cell cycle" gene list were included in this data set. Genes and samples were organized by hierarchical clustering. Relapse-free and overall survivals were calculated as described above.

Centroid Correlation

The method of calculating the centroid for each patient was previously described by Sorlie et al. [28]. The centroids were profiles that consisted of the average gene expression value for each of the patients. Briefly, the centroids for the genes that represented the "tumor-endothelial cell–induced M-phase cell cycle" signature as well as the other signatures were calculated based on the NKI data set. To test a similarity between the signatures, the correlation between values of different centroids was checked for each patient. The correlation was calculated using the Pearson correlation coefficient with R software [29].

Results

Setup of a Tumor-Endothelial Coculture Model

As a model for investigating the gene expression program in response to epithelial-endothelial interactions in the normal breast and in breast cancer, cells that represented either benign or malignant epithelial cell compartments and cells that represented endothelial cell compartments were examined in an *in vitro* mixed coculture setting. The cells were cocultivated for 48 hours in low-serum medium (0.2% FBS) to allow reciprocal signal exchange with minimal background from the influence of undefined molecular signals that are inherent in fetal bovine serum. We examined the effects of cocultivation for each cell pair in two independent biologic replicates. The gene expression profiles of the cocultures were compared with the expression profiles of the corresponding cells that were kept in monoculture using cDNA microarrays that contained approximately 40,700 elements representing 24,472 unique Unigene clusters (build no. 173, released on July 28, 2004). To establish this experimental approach, we first focused our experiments on the breast cancer cell line, Hs578T, the dermal microvascular endothelial cell, HDMEC, and the coculture of these two cell types. The data passing our data quality filter, a filter for data distribution and a filter selecting genes that are more consistent within replicate samples than between experimental samples, were organized using unsupervised hierarchical clustering of the replicate experiments to provide an overview of the effects on global gene expression (Figure 1*A*). In the coculture, most genes displayed intermediate expression levels, which closely approximated the proportionally weighted average of their expression levels in the two cell types in monoculture. Despite setting up the coculture with equal cell numbers of Hs578T and HDMEC, the gene expression pattern after cocultivation is dominated by the pattern of Hs578T. However, one set of genes showed a consistent increase in transcript abundance in the coculture when compared with either monoculture, which suggested that the induction of these genes was an effect of cocultivation.

Interestingly, 11% of the 44 genes within this gene set are involved in DNA replication as determined by GO terms, and they are *RRM2*, *Cdc45L*, *MCM4*, *KIAA1212*, and *MCM8* [26] (Appendix Figure 1). The frequency of the genes that were involved in this function is significantly enriched ($P = .006$) compared with the background of 1140 genes passing the data quality and data distribution filters as shown in the heat map of Figure 1. Furthermore, several genes are involved in the cell cycle, and they are *CCNA2*, *RAD54B*, *AURKA*, and *CENPN*. *STC1*, which is an extracellular matrix protein found in breast cancer [30] and known to be involved in angiogenesis [31], was also detected in this set of genes. Taken together, these gene sets suggest proliferation of the tumor-endothelial cell coculture.

Because breast cancer is a clinically and molecularly heterogeneous disease, we selected a broad spectrum of different breast cancer cell lines to sample this heterogeneity and explore the effects of a heterotypic

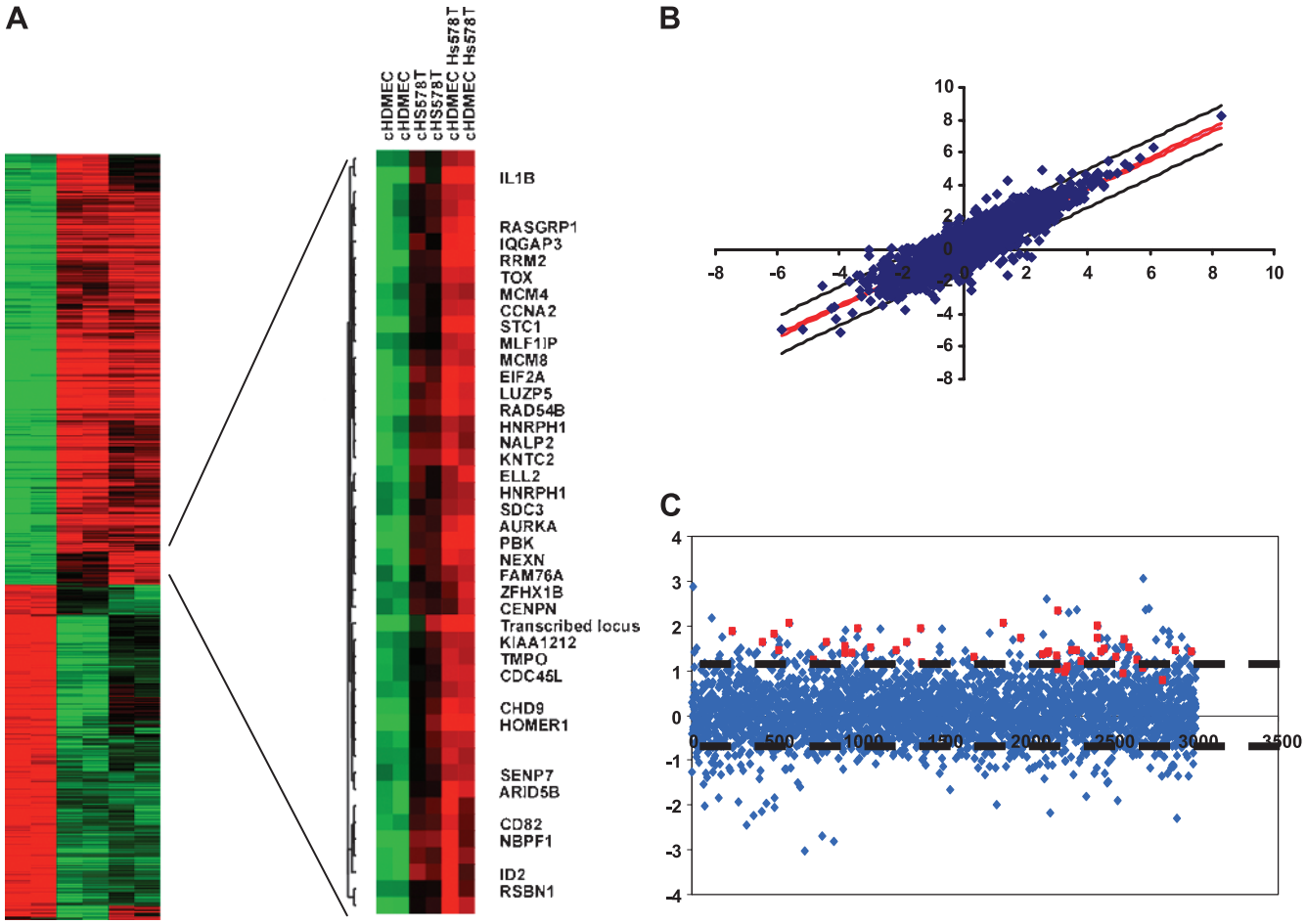

Figure 1. Effect of heterotypic interaction between an endothelial cell and a breast cancer cell line. (A) Biologically independent replicates of the monocultured HDMEC, the breast cancer cell line Hs578T, and the mixed coculture of HDMEC and Hs578T were grown for 48 hours at low serum conditions and characterized by DNA microarray hybridization. Hierarchical clustering of a total of 1140 elements that display a greater than three-fold variance in expression in more than two different experimental samples. Data from individual elements or genes are represented as single rows, and different experiments are shown as columns. Red and green denote the expression levels of the samples. The intensity of the color reflects the magnitude of the deviation from baseline. Unsupervised hierarchical clustering of the experiments grouped the biologic replicates together. Gene expression varied considerably between HDMEC and Hs578T cultures as expected for cells of mesenchymal or epithelial origin, respectively. The coculture profile showed mainly intermediate expression levels. However, the vertical black bar marks a cluster of genes that were induced in all cocultures when compared with both monocultures, which indicated that they were induced by the heterotypic interaction. Zooming in on the genes that were upregulated in coculture revealed that they were specific for proliferation and mitosis. (B) Correlation of the measured coculture gene expression levels and their estimated expression levels based on the proportional contribution of each cell type as determined by a linear regression fit of the monoculture to the coculture data. (C) Fold change of each gene that was associated with coculturing of HDMEC and Hs578T. Genes of the "proliferation and mitosis" cluster are indicated in red. Dashed lines indicate 95% confidence limits.

culture by looking for subtype-specific and shared response patterns. The focus was on epithelial-endothelial cell interactions, which were studied by cocultivating endothelial cells of different origins (HUVEC and HDMEC) in combination with HMECs or six widely used breast cancer cell lines. HDMECs, which are a commercially available dermal microvascular endothelial cell line, were selected to resemble the tumor vasculature endothelial cells of breast cancer as accurately as possible. HUVECs were selected to represent venous cells, despite the fact that the umbilical and breast environments are different. However, the changes that were observed suggest the system works well.

The changes in gene expression that are due to heterotypic interactions were subtle when compared with the large intrinsic variation in expression patterns among the involved cell types, as illustrated in Figure 1*A* for the cell pair of Hs578T and HDMEC. To identify the gene expression changes that resulted from cell-cell interactions, it was necessary to control for the simple additive effects that reflect the proportional contribution of the two cell types to the total population of each gene's transcript in coculture. Elimination of these proportionally weighted additive contributions allowed the isolation of supra-additive interaction effects. The fact that the transcript levels of most genes did not change in response to coculture allowed a linear regression model that was based on the transcription profiles of each monoculture be fitted to the coculture data for normalization. An example of this type of analysis is shown in Figure 1*B*. For each gene, the ratio of the measured transcript level and the level that was estimated by the linear model provides a measure of the heterotypic interaction effect. This is illustrated in Figure 1*C*, which shows the distribution of the gene expression changes of the Hs578T/HDMEC coculture. The genes that

were identified by hierarchical clustering as differentially expressed in coculture when compared with monoculture are highlighted to illustrate the performance of this approach. Interaction effects, which are represented as gene expression changes, are converted to quantitative values that can be analyzed for similarities and disparities over multiple different pairwise interactions between cells with the same tools that are used to analyze conventional gene expression data.

There was an obvious heterogeneity in the responses of different pairs of cells to cocultivation (Figure 2). A striking feature was a cluster of genes that was induced in MDA-MB-231 and Hs578T cocultures with either HUVEC or HDMEC but not in the cocultures with the HMECs. To test for enrichment in a specific functional gene ontology, we applied again the GO::Termfinder tool and found that this set of 104 genes was highly enriched for genes associated with the M-phase of the cell cycle compared with the background of 8140 genes (P = 1.87e – 16). This set of "tumor-endothelial cell–induced M-phase cell cycle" genes included *TOP2A*, *CDC2A*, *CCNB2*, *DHFR*, *CIT*, *TK1*, *CCNA*, *RRM2*, *NUSAP1*, *TPX2*, *CDC25C*, *CENPA*, *CENPE*, *AURKA*, *DTL*, *DICER*, *WHSC1*, *PSIP1*, and *MTPN*. Interestingly, *WHSC1* plays a role in tumorigenicity, adhesion, and clonogenic growth in multiple myeloma [32]; *PSIP1* [33], which is a transcriptional coactivator that is involved in different processes, plays a protective role in stress induced apoptosis; and *MTPN* [34] is a gene that belongs to the myotrophin family.

Differential Induction of Proliferation with Conditioned Medium from Different Tumor Types

As implied by the higher expression of the "tumor-endothelial cell–induced M-phase cell cycle" gene signature, the proliferation rate, as determined by direct cell counting over time, was significantly higher in the coculture of Hs578T and HUVEC than in isolated Hs578T or HUVEC cultures (Figure 3*A*). Also, by flow cytometric cell cycle analysis using propidium iodine staining, we observed a higher proportion of cells leaving the G_1 phase in the coculture than in the monocultures indicative of a higher proportion of cells cycling and passing the M-phase (data not shown).

We speculated that specific factors secreted by the tumors might increase the growth of the endothelial cells or *vice versa*. Toward this aim, we reciprocally incubated one cell type in conditioned medium from the other cell type. In fact, when the conditioned medium from the HUVECs is applied to the tumor cells, the tumor cells show a significantly higher proliferation rate than when kept in autologous medium as measured by the increase in relative cell numbers using the WST-1 proliferation assay (P = 1.3e – 12 [MCF-7], P = 4.6e – 06 [Hs578T], P = 4.3e – 07 [MDA-MB-231], unpaired 2-sided t test; Figure 3*B*). This explains the enhanced proliferation, but it does not explain the differences in proliferation between cocultures of the distinct tumor subtypes. Of note, the conditioned medium from HUVECs induced a higher level of proliferation in MCF-7 cells than in either MDA-MB-231 or Hs578T cells. However, when the conditioned media that are derived from the different tumor types are applied to HUVECs, there is an increase in proliferation on stimulation with conditioned medium from Hs578T cells, which is not seen in the response to the supernatant from MCF-7 cells (Figure 3*C*). This pattern of differential induction is consistent with the differences in the expression of the "tumor-endothelial cell–induced M-phase cell cycle" gene signature, which was observed in the cocultures of Hs578T or MCF-7 in combination with HUVECs.

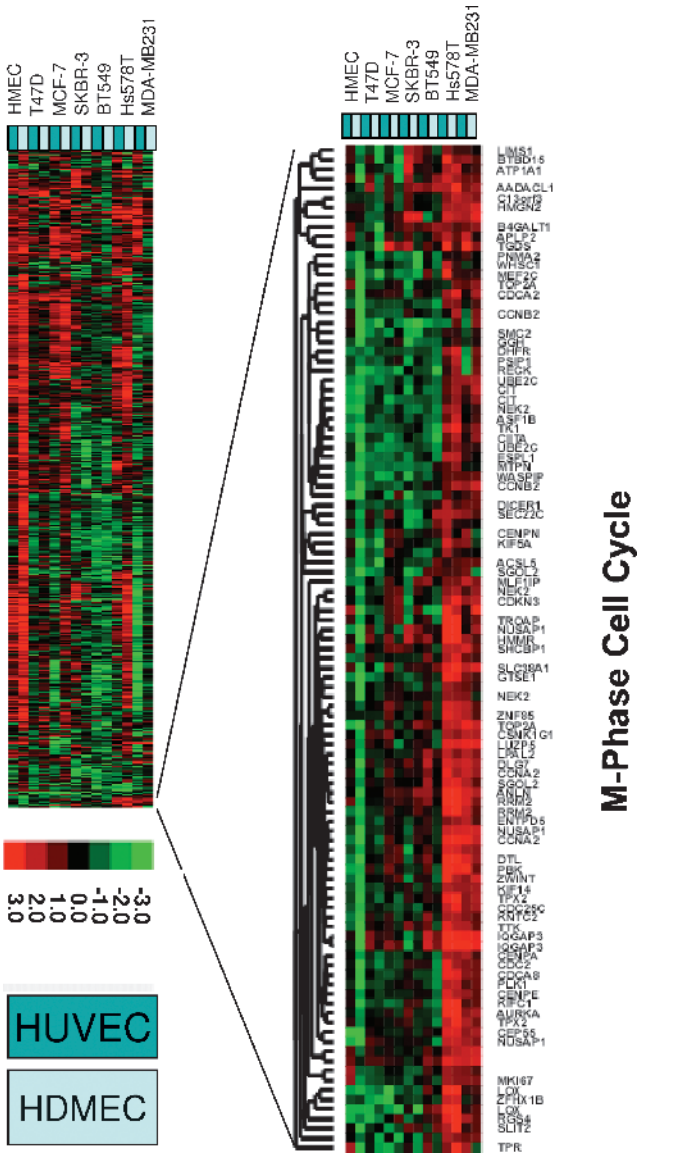

Figure 2. Gene expression changes in multiple cocultures of breast cancer cell lines with endothelial cells. Overview of collapsed data from repeat coculture experiments of eight benign and malignant epithelial cells with two different endothelial cells (HUVEC and HDMEC). The 9 monocultures and the 14 cocultures were analyzed independently in duplicates on 46 HEEBO arrays. Raw data were filtered for technical quality as described in Materials and Methods section, leaving 37,773 spots. A data distribution filter eliminating spots with a $\log_2$-based red-green normalized ratio of less than 1 in at least two arrays removed 10,183 suid(s), leaving 27,590. Genes with missing data in more than 20% of the arrays were removed, leaving 14,565. On the basis of this data set, the calculation of the interaction factors was performed for all 14 cocultures separately as described in Materials and Methods section. The interaction factors were then further analyzed for their distribution, and factors with an SD of less than 0.5 were eliminated, leaving interaction factors for 8140 genes, which are shown as a heat map after unsupervised hierarchical clustering. Red and green denote relative changes in expression that were associated with heterotypic interaction. The magnitude of the relative change is given by color intensity. Zooming in on a cluster of genes that was consistently upregulated in more than two of the cocultures revealed that they were specific for the M-phase of the cell cycle.

Differential Pattern of Secreted Factors in the Tumor Subtypes

We speculated that the induction of the "tumor-endothelial cell–induced M-phase cell cycle" genes in cocultures of Hs578T and MDA-MB-231 is due to cell-cell signaling of factors that are specifically expressed at higher levels in these cells. To systematically identify these molecules, a two-class significance analysis of microarray data was performed [25], with one class formed by Hs578T and MDA-MB-231 and the other by HMEC, HDMEC, HUVEC, BT549, SKBR3, T47D, and MCF-7. Among the genes that were expressed at significantly higher levels in these two cell types were several inducers of angiogenesis, which included *VEGFC*, *FGF12*, *PTN*, and *NF1*. There were also several transcription factors that were coexpressed with these genes, such as *SNAI2* and *ZFHx1B*, which are known to be involved in the epithelial-mesenchymal transition. Interestingly, the PDGFB receptor, which responds to PDGFB that is secreted by endothelial cells, was found in these cells (Figure 4*A*). The full list of genes is given in Appendix Table 1.

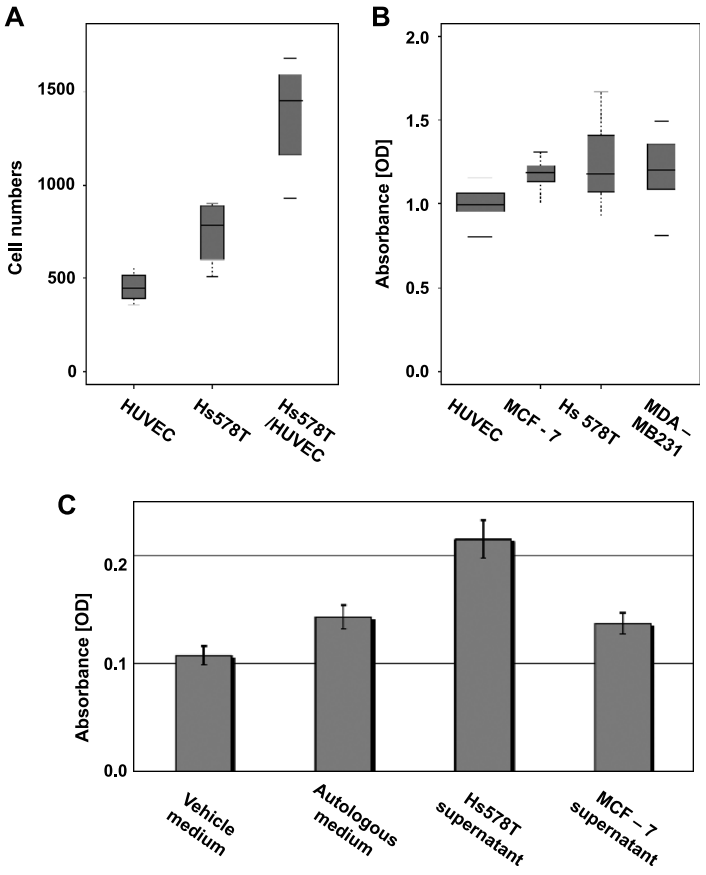

Figure 3. Proliferation of tumor and endothelial cells is due to reciprocal stimulation. (A) Proliferation of HUVECs and Hs578T monocultures and their 1:1 coculture as determined by measuring the increase in cell number by direct cell counting after 36 hours. (B) Box-and-whisker diagrams of relative cell numbers of MCF-7, Hs578T, and MDA-MB-231 after incubation with conditioned medium from HUVECs compared with a normalized negative control of the same cells incubated with autologous medium as measured by the colorimetric cell proliferation assay with the WST-1 compound. (C) Proliferation of HUVECs that was induced by conditioned medium from Hs578T and MCF-7 cells as measured by WST-1. Relative absorbance values of colorful formazan, which has been converted by HUVECs, correspond to relative cell numbers. A single column represents average absorbance values for a minimum of eight independent replicates. *y* Axis error bars correspond to SD. The HUVECs that were treated with the Hs578T supernatant grew significantly faster than the same cells that were treated with the MCF-7 supernatant, the fresh vehicle medium, or the autologous (HUVEC-derived) medium.

Expression of CD44/CD24 in the Diverse Cells

Because breast cancer cells that have the potential to influence the cells within their microenvironment in a way that enhances proliferation might have stem cell characteristics, we speculated that the tumor cells that expressed these angiogenic factors might carry the $CD44^+/CD24^-$ stem cell–like signature, as previously described [35]. Figure 4*B* shows the relative expression of the mRNA of these two antigens in the breast cancer cell lines as measured on the cDNA microarray. CD44 is consistently upregulated in the breast cancer cells that induced the M-phase cell cycle genes in the coculture with endothelial cells, whereas CD24 is consistently downregulated.

This led us to the following working model: Tumor cells first secrete endothelial stimulatory signals, such as VEGF, FGF12, PTN, and NF1 (Figure 4*C*). On stimulation, the endothelial cells start to express PDGFB, which then signals back to the tumor cells through the upregulated PDGFB-R. This feedback loop is facilitated by matching pairs of receptors and ligands, and the coculture starts proliferating.

Blocking Hs578T-Induced Proliferation of HUVEC with Bevacizumab

One of the best described signaling pathways of endothelial cell proliferation is the VEGF pathway [12]. This pathway can be specifically blocked by bevacizumab, which is a monoclonal antibody against VEGF [36]. Whereas Hs578T induces the "tumor-endothelial cell–induced M-phase cell cycle" gene signature in cocultivation with HDMEC, the expression level of this signature in the coculture of MCF-7 and HDMEC represents just the average of the two cells in monoculture (Figure 5*A*). In accordance with these observations, bevacizumab is able to specifically block the stimulatory effect of Hs578T conditioned medium on HUVECs, whereas there was no significant effect on HUVECs that were incubated with conditioned medium that was derived from MCF-7 (Figure 5*B*). Bevacizumab, in contrast to trastuzumab, which served as a negative control, was able to block the conditioned medium that was derived from Hs578T cells and resulted in a reduction in proliferation of HUVECs by approximately 50% to 80%, depending on the antibody concentration (Figure 5*C*). This supports the VEGF pathway as an important factor that enhances tumor-endothelial cell proliferation. However, it is not sufficient alone to explain the full effect. Other factors that were identified by differential expression analysis in our coculture model might also be involved and, therefore, represent valuable targets for therapeutic intervention.

In Vivo *Effects of the "Tumor-Endothelial Cell–Induced M-Phase Cell Cycle" Gene Signature*

We investigated the effect on global gene expression in response to heterotypic cell-cell interaction as a simple, controlled, *ex vivo* model of tumor-endothelial cell interaction. We reasoned that identifying and characterizing gene expression programs that were characteristically induced by the interaction between specific pairs of cells in culture might enable us to recognize and interpret specific features in the expression profiles of human cancers that represent similar interactions between

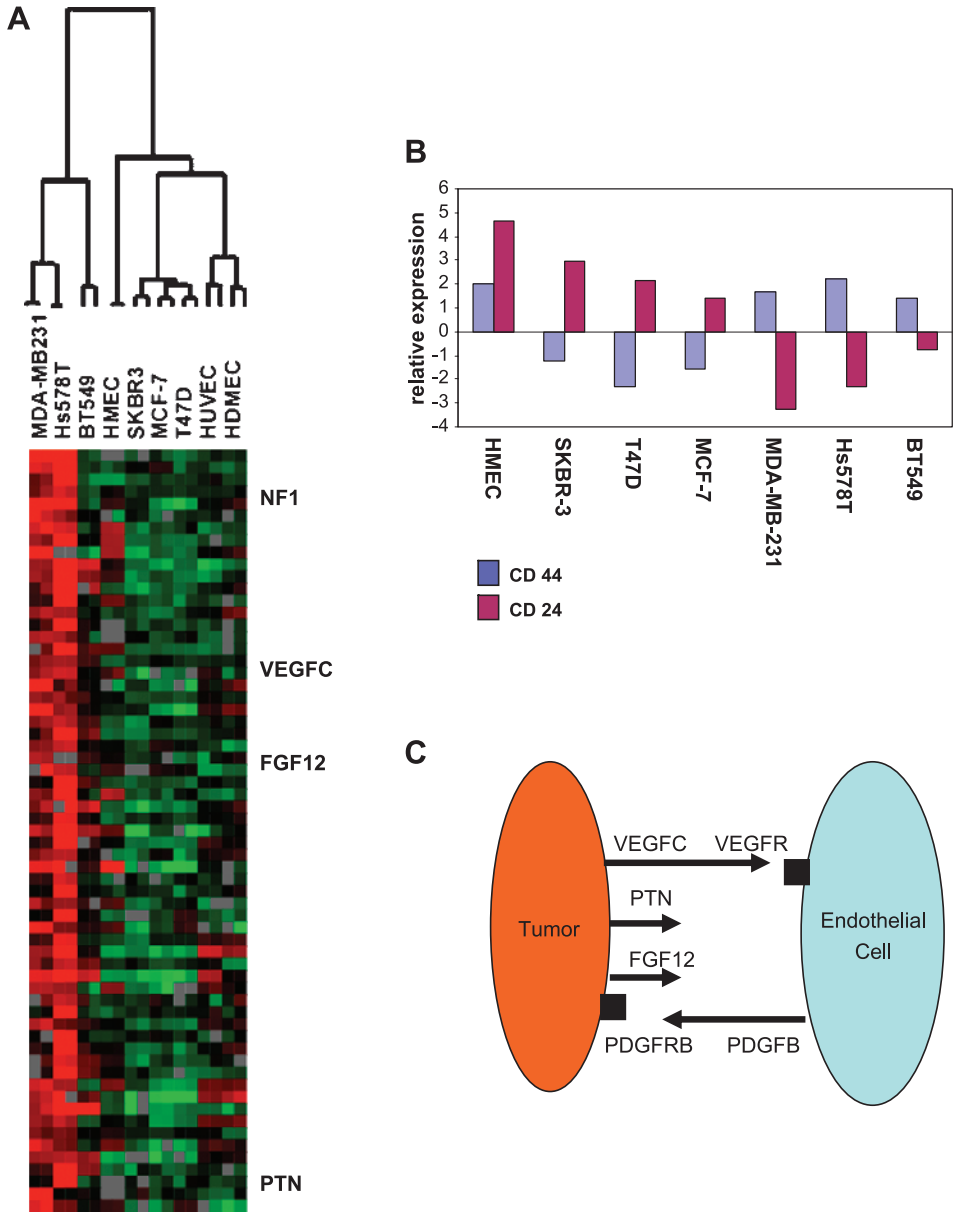

Figure 4. Genes associated with the tumor-endothelial induced M-phase cell cycle gene signature. (A) Significance analysis of microarray data to identify genes that show the largest expression differences between tumor cells that were inducing a proliferation response in coculture with the cells and those that were not inducing proliferation. The expression levels of the top 63 genes are shown on a heat map after unidimensional hierarchical clustering of the genes. (B) Relative expression of CD44 and CD24 in diverse breast cancer cell lines. The average expression of their mRNA over the cell lines corresponds to 0. (C) Working model of reciprocal tumor-endothelial signaling based on the higher expression in the cocultures that induced proliferation.

tumor and endothelial cells *in vivo*. The most consistent response to *ex vivo* cocultivation of breast cancer and endothelial cells was the induction of "tumor-endothelial cell–induced M-phase cell cycle" genes. We, therefore, looked for this response in the expression patterns in the published data from 295 early-stage (stages I and II) breast cancer samples from the NKI [27]. The "tumor-endothelial cell–induced M-phase cell cycle" genes showed a strikingly coherent variation in expression among these cancers, which enabled these cancers to be divided into two groups. One group had a relatively high expression and the other had a relatively low expression of the "tumor-endothelial cell–induced M-phase cell cycle" genes. Clustering the breast carcinomas based only on the expression of the "tumor-endothelial cell–induced M-phase cell cycle" genes separated them into two main clusters, with one cluster having a high-level expression of most of the "tumor-endothelial cell–induced M-phase cell cycle" genes and the other having a lower expression of these genes (Figure 6*A*). The same coordinated behavior and segregation of tumors could be observed in a different set of advanced breast cancer samples [28,37], which suggested that variation in this "tumor-endothelial cell–induced cell M-phase cell cycle" program is a general feature in breast cancer (Appendix Figure 2).

As a first assessment of its potential biologic relevance, distant metastasis-free survival and overall disease-specific survival were compared between the two groups. Early-stage tumors with high expression

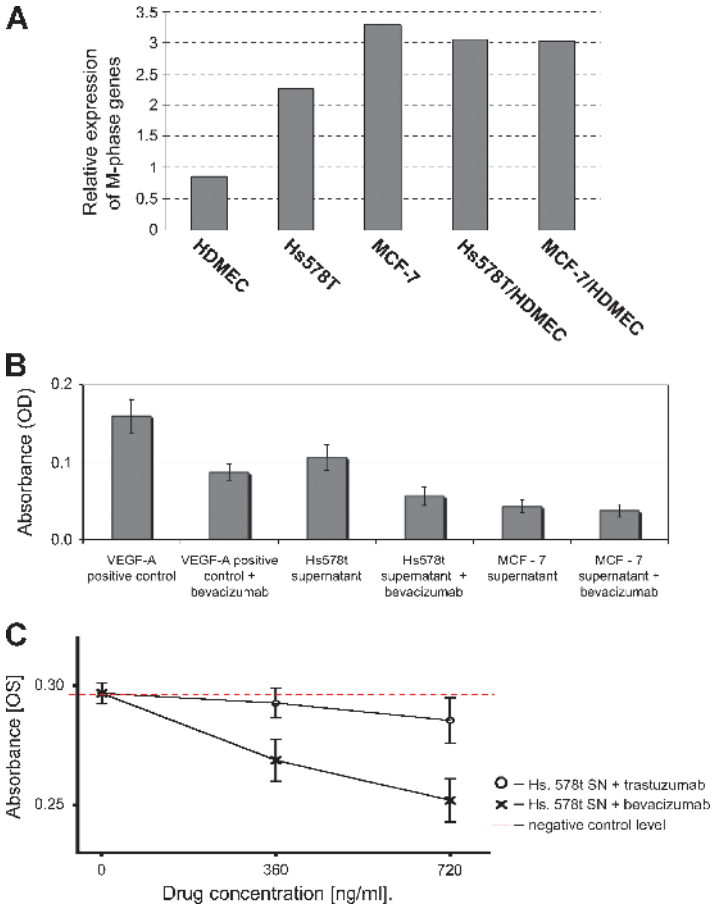

Figure 5. Stimulatory effect of Hs578T conditioned medium on endothelial cells can be partially blocked by bevacizumab. (A) Relative expression of the "tumor-endothelial cell–induced M-phase cell cycle" genes in different monocultures of breast cancer cell lines and endothelial cells and in their respective cocultures. (B) Blocking of the stimulatory effect of Hs578T conditioned medium by bevacizumab. Absolute absorbance values of formazan dye that was converted by HUVECs, which corresponds to cell numbers, are shown in columns, with the *y* axis bars corresponding to SD. Bevacizumab (100 ng/ml) depleted the stimulatory effect of Hs578T cell culture supernatant in a significant manner, whereas it had no effect on the MCF-7 cell culture supernatant. Recombinant VEGF-A (5 ng/ml) and 5% FBS served as positive and negative controls, respectively. (C) Dose-dependent blocking of HUVEC proliferation by bevacizumab and trastuzumab. Absolute absorbance values of formazan dye that was converted by HUVECs are shown. HUVECs that were treated with the Hs578T cell culture supernatant represent the baseline stimulatory effect. Bevacizumab depleted the stimulatory effect of the Hs578T conditioned medium in a significant, dose-dependent manner. Trastuzumab, which is a monoclonal antibody against HER2, did not influence HUVEC stimulation by the Hs578T conditioned medium.

levels (n = 137) of this particular gene set had a significantly lower distant metastasis-free survival (P = 1.8e – 5; 50% at 10 years) and overall survival rate (P = 5e – 9; 52% at 10 years) than tumors with low expression levels (n = 158; metastasis-free survival, 73% at 10 years; overall survival, 84% at 10 years; Figure 6*B*).

The same trend toward unfavorable outcome in patients with cancers that showed high levels of "tumor-endothelial cell–induced M-phase cell cycle" gene transcripts (P = .17) could be seen in the analysis of the data set from advanced-stage breast cancers [28] (data not shown) from Norway/Stanford.

Correlation to Other Prognostic Gene Expression Signatures

The relationship between the "tumor-endothelial cell–induced M-phase cell cycle" gene signature and three previously identified gene expression signatures, which were useful prognosticators in this data set, were also investigated (Figure 7). The first signature is a set of 70 genes [38], which was identified in a supervised analysis of a subset of the NKI early-stage breast cancer data set [27], that could predict freedom from metastasis at 5 years. The second signature was identified *in vitro* by exposing fibroblasts to serum to mimic a wound response, and it has been shown to predict a risk of progression [39]. The "tumor-endothelial cell–induced M-phase cell cycle" gene signature seems to be highly correlated with the poor prognosticator wound (0.605) signature and to be the reciprocal of the good prognosticator 70-gene signature (–0.708), which indicated that our hypothesis that was based

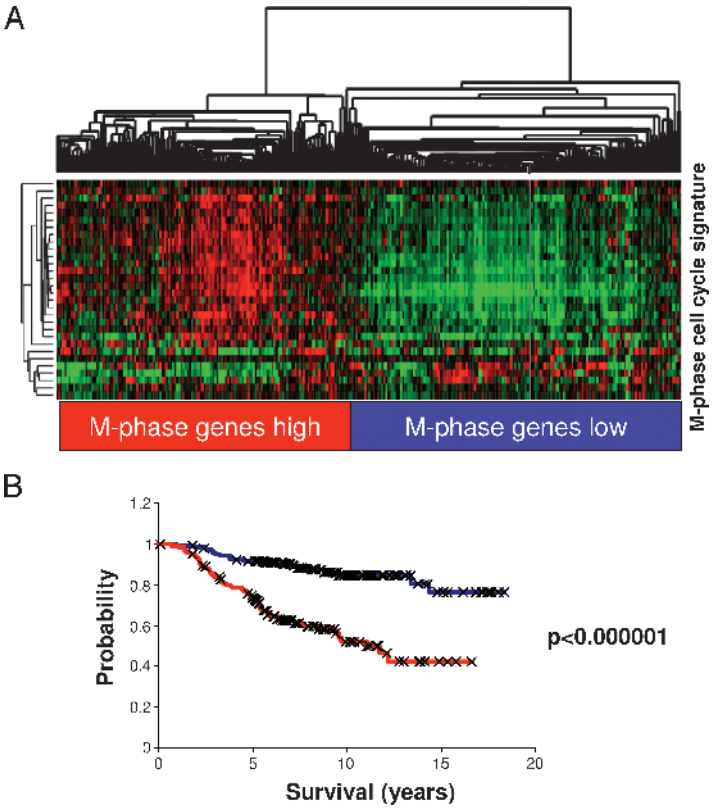

Figure 6. "Tumor-endothelial cell–induced M-phase cell cycle" genes in early-stage breast cancer. (A) The expression values of genes in the "tumor-endothelial cell–induced M-phase cell cycle" gene signature were extracted from a published expression study of 295 early-stage breast cancers from the Netherlands Cancer Institute [35]. Genes and samples are organized by hierarchical clustering. The tumors were segregated into two groups that were defined by high (red) or low (blue) expression levels of the 30 genes matching the M-phase cell cycle gene cluster. (B) Correlation of the "tumor-endothelial cell–induced M-phase cell cycle" gene signature status with distant metastasis-free and overall survival. Kaplan-Meier curves for the clinical outcomes of the indicated tumors that exhibit high (red curve) and low (blue curve) "tumor-endothelial cell–induced M-phase cell cycle" gene signature expression are shown.

on an *in vitro* model is of *in vivo* clinical relevance. Interestingly, the "tumor-endothelial cell–induced M-phase cell cycle" gene signature has even a higher correlation to the 70-gene profile, which was derived as a prognosticator by a top down analysis of this exact data set, than the wound signature. The invasiveness gene signature, which was derived from a comparison of $CD44^+/CD24^-$ stem cell–like cells with normal breast epithelial cells, predicted poor prognosis in breast cancer [40]. This signature, despite having similar prognostic power as the wound signature, did not correlate well with the 70-gene signature, with the wound signature, or with the "tumor-endothelial cell–induced M-phase cell cycle" gene signature (–0.21).

Discussion

The main objective of this study was to examine and characterize the effects of heterotypic cellular interaction to gain insight into the underlying biology of these effects in normal mammary tissue and in breast cancer, with a specific focus on the interaction between epithelial tumor cells and endothelial cells. To isolate specific, direct interactions from more complex interactions that involve multiple cell types in a whole tissue or organism, we used a simple *ex vivo* coculture model. Because some important heterotypic interactions might require direct cell-cell contact, we focused on a coculture model where the two cell types were mixed [22]. In this report, we describe the systematic genomic analysis

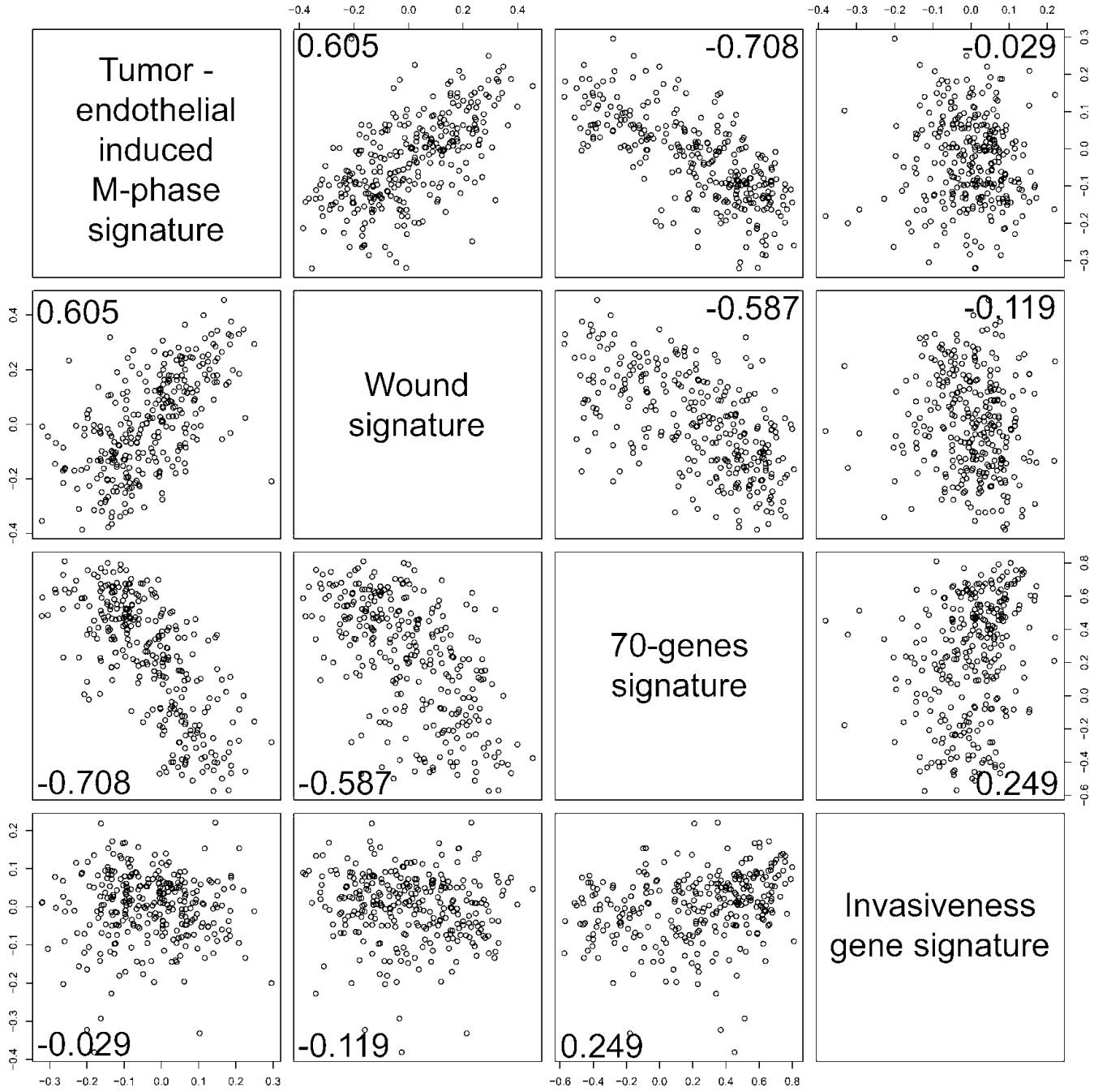

Figure 7. Correlation to other prognostic gene signatures in early-stage breast cancer. Correlation of the 70-gene signature [50], the wound signature [49], the invasiveness gene signature [40], and the "tumor-endothelial cell–induced M-phase cell cycle" signature score in the NKI data set. Pairwise scatter plot matrix of the three gene signatures. Pearson correlations are shown in the lower part of each plot.

of this simple *in vitro* system that simulates direct and indirect interactions between benign and malignant epithelial cells and endothelial cells in normal breast tissue and in breast cancer.

Common Gene Set Induced by Tumor-Endothelial Coculture

As expected, based on our experience with the tumor-fibroblast interaction [22], the picture of heterotypic interaction effects from the survey of diverse tumor cells with two different types of endothelial cells is complex and reflects the different abilities of normal and malignant cells to send and respond to extrinsic signals. Our data show that the effects of the tumor-endothelial cell interaction differ between different breast cancer cell lines that each represents a different breast cancer subtype. A prominent theme in our coculture experiments was a set of genes that were characteristic of the mitotic phase of the cell cycle, which we called the "tumor-endothelial cell–induced M-phase cell cycle" gene expression signature. This observation on the gene expression level is consistent with the phenotypic features that show a higher proliferation rate in the respective cocultures. In our setting, the mere coexistence of two cell types of different origin, such as the Hs578T breast cancer cells and endothelial cells, seems to be sufficient to induce proliferation. Cooperate induction between cells of different lineages is well known from developmental biology, where stem cells cooperate with their environmental cells to form the stem cell niche. The stem cell concept has also been introduced in cancer [41]. Cells with stem cell characteristics have been prospectively isolated from breast cancer using CD44 and CD24 as markers [35]. From these cells, which are characterized as $CD44^+/CD24^-$, a prognostic gene expression signature has been determined, which has been called the invasiveness signature [40]. This signature has been associated with an unfavorable prognosis in breast cancer. However, it was unclear how that small fraction of stem cells could lead to such a prominent gene expression pattern in the genomic profile of breast cancer, and it was unexpected that a signature that was derived from stem cells, which are known for their low proliferative potential, was linked to the highly proliferative, poor prognostic tumors.

Hs578T and MDA-MB-231 both exhibit the $CD44^+/CD24^-$ phenotype. Whereas in monoculture under low serum conditions, they proliferated slowly in a manner that was similar to stem cells [42,43], in coculture with endothelial cells, they had a high proliferation rate along with associated changes in gene expression. This induction of proliferation markers is absent in the cocultures with $CD44^-/CD24^+$ cells. Therefore, cocultivation of endothelial cells with breast cancer cells links the $CD44^+/CD24^-$ signature with high proliferation, which is then associated with the overexpression of the "tumor-endothelial cell–induced M-phase cell cycle" gene signature and predicts a poor prognosis in breast cancer. We are well aware that the $CD44^+/CD24^-$ signature is preferentially associated with basal type carcinomas, in contrast to the $CD44^-/CD24^+$ signature, which is associated with the luminal-type breast cancer cells [44]. In this context, the cocultivation with endothelial cells explains the worse prognosis of basal type breast cancer despite the lower proliferation rate of the isolated basal-type breast cancer cells in monoculture. This exemplifies that this simple *in vitro* coculture model is more similar to the *in vivo* situation than the monoculture. The stem cell–like cells with highly potent tumor-initiating properties, as they were described by Al-Hajj et al. [35], clearly exhibited the $CD44^+/CD24^-$ signature but were also characterized by additional markers. It has been shown that $CD44^+/CD24^-$–expressing cell lines contain these tumor-initiating cells [42,45], but, of note, we did neither specifically focus on nor explicitly select for these stem cell–like cells.

Differences Are Due to Differential Endothelial Cell Proliferation

A comparison of the gene expression program between the $CD44^+/CD24^-$ tumor cells that upregulate the "tumor-endothelial cell–induced M-phase cell cycle" genes and the $CD44^-/CD24^+$ tumor cells that do not reveals multiple genes that seem to be involved in angiogenesis. This gene subset includes *VEGF*, *FGF*, and other endothelial stimulatory factors. Many genes in this cluster are functionally less well described, although they might be involved in tumor cell proliferation or in the induction of tumor angiogenesis. To demonstrate their functional impact, we blocked VEGF with bevacizumab, which is a specific antibody against VEGF. A good part of the stimulatory effect of Hs578T conditioned medium on HUVECs was abrogated with bevacizumab. This demonstrates that these genes play a considerable functional role and are not just surrogate markers that are associated with faster tumor growth. Whereas VEGF partially blocks the effects of the tumor cell supernatant, other factors might also contribute to endothelial proliferation and thereby represent possible additional new therapeutic targets. Most notably, these additional factors could be responsible for drug resistance to anti-VEGF monotherapy if tumors start using these alternative angiogenic factors to grow blood vessels.

With consideration to the cancer stem cell concept, the stem cell niche has been proposed to play an important role in carcinogenesis and progression, although it remains largely uncharacterized at the cellular and molecular levels. It is possible to speculate that endothelial cells participate in the breast cancer stem cell niche. In a mouse model, $VEGFR^+$ bone marrow–derived cells have been shown to form a stem cell niche for cancer cells, and such cells have been identified in human breast cancer biopsies [46]. In brain cancer, stem cells were demonstrated to live in a vascular niche that secretes factors that promote their long-term growth and self-renewal [47]. The factors that we have described to enhance the proliferation of Hs578T, a $CD44^+/CD24^-$–expressing cell line, which contains at least in part stem cell–like cells [42] and endothelial cells, might also be involved in a breast cancer stem cell niche. We are well aware that the endothelial cells of the vascular system are diverse [48] and that the tumor vasculature consists of specifically altered endothelial cells. The endothelial cells that we selected, which were the HUVECs and HDMECs, do not represent the autologous tumor vasculature endothelial cells of breast carcinomas. We can, therefore, not exclude the possibility that endothelial cells that are isolated from within a tumor might show additional specific interaction effects. Nevertheless, it would be surprising if carcinoma-associated endothelial cells failed to show the strong effects that we consistently observed in cocultures with HUVECs and HDMECs. Because these experiments might be insufficient to detect subtle differences between cocultures that involve different types of tumor-endothelial cells, a more specific selection of primary tumor-associated endothelial cells would be needed in the optimal case in cocultivation with primary tumor cells.

Predictive Marker for Antiangiogenic Drugs

We have shown that the "tumor-endothelial cell–induced M-phase cell cycle" signature is a strong prognostic signature that strongly correlates with other prognostic signatures such as the wound signature [49] and the 70-gene signature [27]. A subset of the genes that are found in our signature overlaps with a subset of the genes that are found in the "wound signature," which was characterized by the stimulation of

fibroblasts with serum, resembling the response of fibroblasts to wounding. Our situation also resembles the situation of wounding, where new vessels have to spread to the wound area to nourish the new wound fibroblasts. The 70-gene signature is currently studied in prospective clinical trials to spare some women chemotherapy without risking their chance of cure [50]. For clinical decision making, it is important to define biomarkers that could serve as predictive factors about the benefit of certain therapies, especially in the case of new therapeutic options, such as antiangiogenic drugs. So far, there is no valid biomarker for this purpose. Although there is evidence from preclinical studies, we have to be cautious when extrapolating preclinical data to the human disease. Preclinical experiments are often designed to look at the influence of well-defined biologic phenomena on drug efficacy. By contrast, human disease is more complex and might require multiple markers to accurately predict efficacy. For this purpose, a set of *in vitro*–designed biomarkers, which are already independently tested for their prognostic power, such as our "tumor-endothelial cell–induced M-phase cell cycle" gene signature or the associated set of angiogenesis-inducing factors, could serve as potential predictors that are worth further evaluation. Our *in vitro* model, which involves the mere coculture of two cell types, seems to allow the identification of a strongly prognostic gene signature. Whereas the genes from the 70-gene signature have not yet been associated with a single functional ontology, our signature is linked to a mechanistic *in vitro* model that allows for further experimentation.

In our previous work, we have modeled the interaction of tumor cells with fibroblasts, which allowed us to define an interferon response gene set [22]. In this work, we have characterized a tumor-endothelial cell interaction. It would be interesting to see how different carcinoma-associated fibroblasts and endothelial cells interact and how the addition of tumor cells would reprogram the system. Our coculture technique may allow us to further explore these more complex interactions among the multiple molecules that operate in these cells to orchestrate the process of cancer progression and metastasis. Our experience suggests that *in vitro* modeling of specific processes and features of the tumor microenvironment can provide a valuable interpretive framework for the analysis of associated gene expression patterns in more heterogeneous *in vivo* samples and the identification of the effects of heterotypic cellular interactions.

Appendix

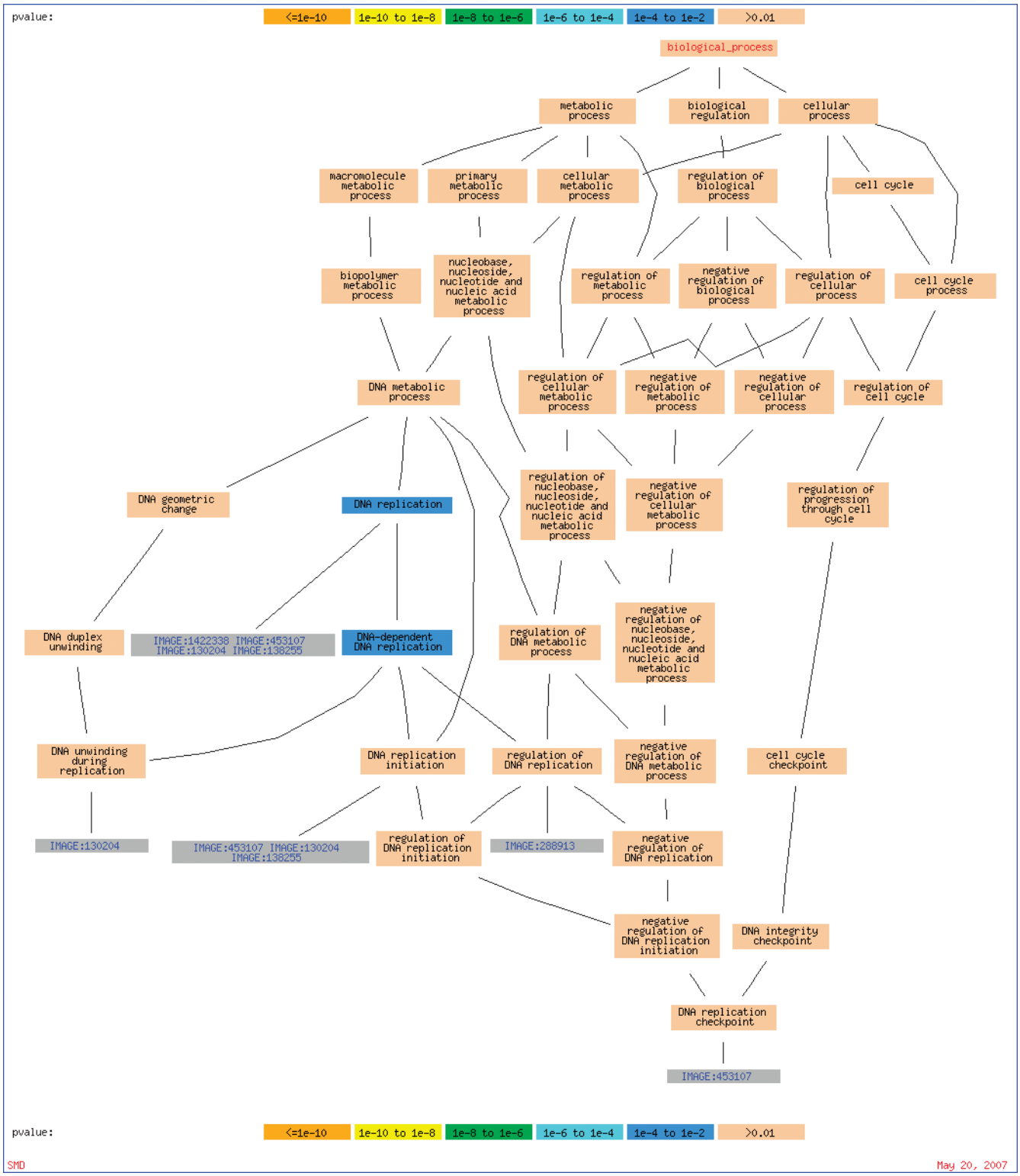

Appendix Figure 1. GO terms. Graphical visualization of the output from GO::Termfinder for process ontology: GOgraph layout that includes the significant GO nodes annotated by DNA replication, derived from 44 clones from a background of 1140. The color of the nodes is an indication of their Bonferroni corrected *P* value (orange $\leq$ 1e $-$ 10; yellow = 1e $-$ 10 to 1e$-$8; green = 1e$-$8 to 1e$-$6; cyan = 1e$-$6 to 1e$-$4; blue = 1e$-$4 to 1e$-$2; tan $>$ 0.01).

Appendix Table 1. List of Genes Expressed in Breast Cancer Cell Lines Inducing Proliferation in Coculture.

CLID	UniGene Cluster ID || Symbol || Gene Name
IMAGE:754582	|| Hs.567266 || *NF1* || Neurofibromin 1 (neurofibromatosis, von Recklinghausen disease, Watson disease)
IMAGE:280699	|| Hs.563491 || *EPDR1* || Ependymin related protein 1 (zebrafish)
IMAGE:138991	|| Hs.233240 || *COL6A3* || Collagen, type VI, alpha 3
IMAGE:878836	|| || || AA670429 || || || IMAGE:878836 || 110839
IMAGE:45138	|| Hs.435215 || *VEGFC* || Vascular endothelial growth factor C
IMAGE:1031532	|| Hs.226780 || *OSTM1* || Osteopetrosis associated transmembrane protein 1
IMAGE:460002	|| Hs.269027 || *GALNT5* || UDP-*N*-acetyl-alpha-D-galactosamine:polypeptide *N*-acetylgalactosaminyltransferase 5 (GalNAc-T5)
IMAGE:204737	|| Hs.360174 || *SNAI2* || Snail homolog 2 (*Drosophila*)
IMAGE:1913366	|| Hs.128013 || *PRSS3* || Protease, serine, 3 (mesotrypsin)
IMAGE:898218	|| Hs.450230 || *IGFBP3* || Insulin-like growth factor binding protein 3
IMAGE:489519	|| Hs.297324 || *TIMP3* || TIMP metallopeptidase inhibitor 3 (Sorsby fundus dystrophy, pseudoinflammatory)
IMAGE:489089	|| Hs.474053 || *COL6A1* || Collagen, type VI, alpha 1
IMAGE:488404	|| Hs.27621 || || Clone TUA8 Cri-du-chat region mRNA
IMAGE:753587	|| Hs.167741 || *BTN3A3* || Butyrophilin, subfamily 3, member A3
IMAGE:857640	|| Hs.420269 || *COL6A2* || Collagen, type VI, alpha 2
IMAGE:1030805	|| Hs.458623 || || Transcribed locus, moderately similar to XP_509196.1 PREDICTED: similar to FTO protein [Pan troglodytes]
IMAGE:868212	|| Hs.369397 || *TGFBI* || Transforming growth factor, beta-induced, 68 kDa
IMAGE:2545711	|| Hs.592971 || || Transcribed locus
IMAGE:1470128	|| Hs.411391 || LOC399959 || Hypothetical gene supported by BX647608
IMAGE:121981	|| Hs.419240 || *SLC2A14* || Solute carrier family 2 (facilitated glucose transporter), member 14
IMAGE:1893136	|| Hs.596112 || || Transcribed locus || AI278518 || || || IMAGE:1893136 || 313617
IMAGE:753467	|| Hs.419240 || *SLC2A14* || Solute carrier family 2 (facilitated glucose transporter), member 14
IMAGE:789147	|| Hs.511915 || *ENO2* || Enolase 2 (gamma, neuronal)
IMAGE:299539	|| Hs.584758 || *FGF12* || Fibroblast growth factor 12
IMAGE:471196	|| Hs.111577 || *ITM2C* || Integral membrane protein 2C
IMAGE:504761	|| Hs.374774 || *ANKRD29* || Ankyrin repeat domain 29
IMAGE:811000	|| Hs.514535 || *LGALS3BP* || Lectin, galactoside-binding, soluble, 3 binding protein
IMAGE:153646	|| Hs.172928 || *COL1A1* || Collagen, type I, alpha 1
IMAGE:897768	|| Hs.476218 || *COL7A1* || Collagen, type VII, alpha 1 (epidermolysis bullosa, dystrophic, dominant and recessive)
IMAGE:263716	|| Hs.474053 || *COL6A1* || Collagen, type VI, alpha 1
IMAGE:269425	|| Hs.34871 || *ZFHX1B* || Zinc finger homeobox 1b
IMAGE:754106	|| Hs.297324 || *TIMP3* || TIMP metallopeptidase inhibitor 3 (Sorsby fundus dystrophy, pseudoinflammatory)
IMAGE:809719	|| Hs.477128 || *CCDC80* || Coiled-coil domain containing 80
IMAGE:1558164	|| Hs.89901 || *PDE4A* || Phosphodiesterase 4A, cAMP-specific (phosphodiesterase E2 dunce homolog, *Drosophila*)
IMAGE:293339	|| Hs.360174 || *SNAI2* || Snail homolog 2 (*Drosophila*)
IMAGE:291290	|| Hs.558402 || *SSX4* || Synovial sarcoma, X breakpoint 4
IMAGE:609332	|| Hs.409662 || *COL14A1* || Collagen, type XIV, alpha 1 (undulin)
IMAGE:239256	|| Hs.173859 || *FZD7* || Frizzled homolog 7 (*Drosophila*)
IMAGE:210717	|| Hs.1501 || *SDC2* || Syndecan 2 (heparan sulfate proteoglycan 1, cell surface-associated, fibroglycan)
IMAGE:415122	|| Hs.48384 || *HS3ST3B1* || Heparan sulfate (glucosamine) 3-*O*-sulfotransferase 3B1
IMAGE:625234	|| Hs.642759 || *KDELR3* || KDEL (Lys-Asp-Glu-Leu) endoplasmic reticulum protein retention receptor 3
IMAGE:843222	|| Hs.210283 || *COL5A1* || Collagen, type V, alpha 1
IMAGE:234736	|| Hs.514746 || *GATA6* || GATA binding protein 6
IMAGE:80643	|| Hs.482730 || *EDIL3* || EGF-like repeats and discoidin I-like domains 3
IMAGE:502689	|| Hs.632387 || *NEXN* || Nexilin (F actin binding protein)
IMAGE:109424	|| Hs.103110 || *PPARA* || Peroxisome proliferative activated receptor, alpha
IMAGE:813823	|| Hs.406475 || *LUM* || Lumican
IMAGE:110503	|| Hs.480712 || *LARP2* || La ribonucleoprotein domain family, member 2
IMAGE:1475595	|| Hs.75431 || *ALPL* || Alkaline phosphatase, liver/bone/kidney
IMAGE:742125	|| Hs.65436 || *LOXL1* || Lysyl oxidase-like 1
IMAGE:510729	|| Hs.437040 || *PTPN21* || Protein tyrosine phosphatase, non-receptor type 21
IMAGE:769686	|| Hs.643513 || *THY1* || Thy-1 cell surface antigen
IMAGE:144916	|| Hs.62661 || *GBP1* || Guanylate binding protein 1, interferon-inducible, 67 kDa
IMAGE:345849	|| Hs.102267 || *LOX* || Lysyl oxidase
IMAGE:502664	|| Hs.35861 || *TMEM158* || Ras-induced senescence 1
IMAGE:786265	|| Hs.501928 || *MICAL2* || Microtubule associated monoxygenase, calponin and LIM domain containing 2
IMAGE:590759	|| Hs.105269 || *SC4MOL* || Sterol-C4-methyl oxidase-like
IMAGE:854678	|| Hs.567598 || *LBH* || Hypothetical protein DKFZp566J091
IMAGE:344272	|| Hs.9999 || *EMP3* || Epithelial membrane protein 3
IMAGE:361974	|| Hs.371249 || *PTN* || Pleiotrophin (heparin binding growth factor 8, neurite growth-promoting factor 1)
IMAGE:1593317	|| Hs.509067 || *PDGFRB* || Platelet-derived growth factor receptor, beta polypeptide
IMAGE:756372	|| Hs.438823 || *KCNH2* || Potassium voltage-gated channel, subfamily H (eag-related), member 2
IMAGE:415134	|| Hs.632256 || *STAT5B* || Signal transducer and activator of transcription 5B

Genes that are differentially expressed between breast cancer cell lines inducing the "tumor-endothelial cell–induced M-phase cell cycle" gene signature contain multiple endothelial growth factors.

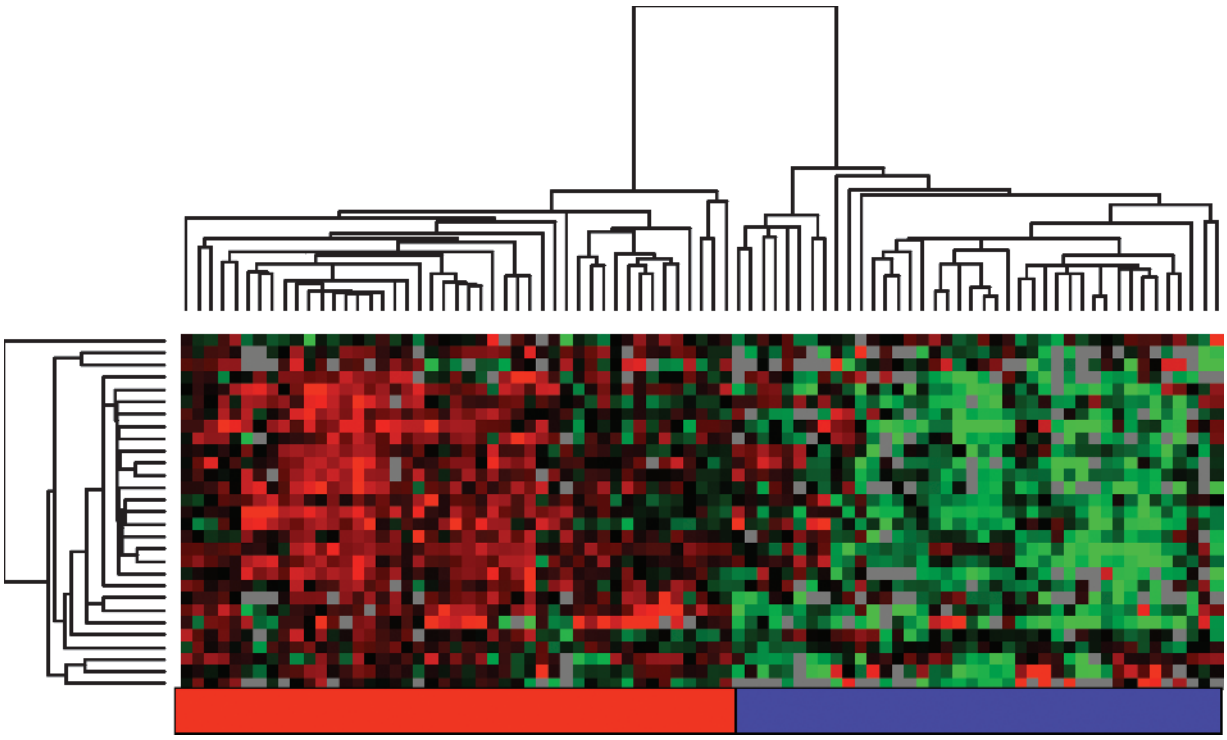

Appendix Figure 2. "Tumor-endothelial cell–induced M-phase cell cycle" genes in advanced-stage breast cancer. The expression values of genes in the "tumor-endothelial cell–induced M-phase cell cycle" gene signature were extracted from a published expression study of advanced-stage breast cancers from Norway/Stanford [33]. Genes and samples are organized by hierarchical clustering. The tumors segregated into two groups defined by high (red) or low (blue) expression levels of 29 genes matching the "tumor-endothelial cell–induced M-phase cell cycle" gene signature.

Acknowledgments

The authors thank Michael Fero, Elena Seraia, and the staff of the Stanford Functional Genomics Facility for supplying the human cDNA microarrays that were used for this study. The authors thank Kathy Ball, Janos Demeter, and the staff from the Stanford Microarray Database for support with the microarray data storage and analysis tools. M.B. is a fellow of the Schoenmakers-Müller Foundation, Basel, Switzerland.

References

[1] Folkman J (1995). Angiogenesis in cancer, vascular, rheumatoid and other disease. *Nat Med* **1**, 27–31.

[2] Folkman J and Shing Y (1992). Angiogenesis. *J Biol Chem* **267**, 10931–10934.

[3] Paweletz N and Knierim M (1989). Tumor-related angiogenesis. *Crit Rev Oncol Hematol* **9**, 197–242.

[4] Fidler IJ and Ellis LM (1994). The implications of angiogenesis for the biology and therapy of cancer metastasis. *Cell* **79**, 185–188.

[5] Kerbel R and Folkman J (2002). Clinical translation of angiogenesis inhibitors. *Nat Rev Cancer* **2**, 727–739.

[6] Yang JC, Haworth L, Sherry RM, Hwu P, Schwartzentruber DJ, Topalian SL, Steinberg SM, Chen HX, and Rosenberg SA (2003). A randomized trial of bevacizumab, an anti–vascular endothelial growth factor antibody, for metastatic renal cancer. *N Engl J Med* **349**, 427–434.

[7] Hurwitz H, Fehrenbacher L, Novotny W, Cartwright T, Hainsworth J, Heim W, Berlin J, Baron A, Griffing S, Holmgren E, et al. (2004). Bevacizumab plus irinotecan, fluorouracil, and leucovorin for metastatic colorectal cancer. *N Engl J Med* **350**, 2335–2342.

[8] Sandler A, Gray R, Perry MC, Brahmer J, Schiller JH, Dowlati A, Lilenbaum R, and Johnson D (2006). Paclitaxel-carboplatin alone or with bevacizumab for non–small-cell lung cancer. *N Engl J Med* **355**, 2542–2550.

[9] Escudier B, Pluzanska A, Koralewski P, Ravaud A, Bracarda S, Szczylik C, Chevreau C, Filipek M, Melichar B, Bajetta E, et al. (2007). Bevacizumab plus interferon α-2a for treatment of metastatic renal cell carcinoma: a randomised, double-blind phase III trial. *Lancet* **370**, 2103–2111.

[10] Miller K, Wang M, Gralow J, Dickler M, Cobleigh M, Perez EA, Shenkier T, Cella D, and Davidson NE (2007). Paclitaxel plus bevacizumab *versus* paclitaxel alone for metastatic breast cancer. *N Engl J Med* **357**, 2666–2676.

[11] Rak J, Filmus J, and Kerbel RS (1996). Reciprocal paracrine interactions between tumour cells and endothelial cells: the "angiogenesis progression" hypothesis. *Eur J Cancer* **32A**, 2438–2450.

[12] Ferrara N, Houck K, Jakeman L, and Leung DW (1992). Molecular and biological properties of the vascular endothelial growth factor family of proteins. *Endocr Rev* **13**, 18–32.

[13] O'Reilly MS, Boehm T, Shing Y, Fukai N, Vasios G, Lane WS, Flynn E, Birkhead JR, Olsen BR, and Folkman J (1997). Endostatin: an endogenous inhibitor of angiogenesis and tumor growth. *Cell* **88**, 277–285.

[14] Compagni A, Wilgenbus P, Impagnatiello MA, Cotten M, and Christofori G (2000). Fibroblast growth factors are required for efficient tumor angiogenesis. *Cancer Res* **60**, 7163–7169.

[15] Ergun S, Kilik N, Ziegeler G, Hansen A, Nollau P, Gotze J, Wurmbach JH, Horst A, Weil J, Fernando M, et al. (2000). CEA-related cell adhesion molecule 1: a potent angiogenic factor and a major effector of vascular endothelial growth factor. *Mol Cell* **5**, 311–320.

[16] Akhta N, Carlso S, Pesarini A, Ambulos N, and Passaniti A (2001). Extracellular matrix–derived angiogenic factor(s) inhibit endothelial cell proliferation, enhance differentiation, and stimulate angiogenesis *in vivo*. *Endothelium* **8**, 221–234.

[17] Bissell MJ and Radisky D (2001). Putting tumours in context. *Nat Rev Cancer* **1**, 46–54.

[18] Bissell MJ, Radisky DC, Rizki A, Weaver VM, and Petersen OW (2002). The organizing principle: microenvironmental influences in the normal and malignant breast. *Differentiation* **70**, 537–546.

[19] Perou CM, Sorlie T, Eisen MB, van de Rijn M, Jeffrey SS, Rees CA, Pollack JR, Ross DT, Johnsen H, Akslen LA, et al. (2000). Molecular portraits of human breast tumours. *Nature* **406**, 747–752.

[20] Teicher BA (1994). Hypoxia and drug resistance. *Cancer Metastasis Rev* **13**, 139–168.
[21] Li L and Neaves WB (2006). Normal stem cells and cancer stem cells: the niche matters. *Cancer Res* **66**, 4553–4557.
[22] Buess M, Nuyten DS, Hastie T, Nielsen T, Pesich R, and Brown PO (2007). Characterization of heterotypic interaction effects *in vitro* to deconvolute global gene expression profiles in cancer. *Genome Biol* **8**, R191.
[23] Demeter J, Beauheim C, Gollub J, Hernandez-Boussard T, Jin H, Maier D, Matese JC, Nitzberg M, Wymore F, Zachariah ZK, et al. (2007). The Stanford Microarray Database: implementation of new analysis tools and open source release of software. *Nucleic Acids Res* **35**, D766–D770.
[24] Eisen MB, Spellman PT, Brown PO, and Botstein D (1998). Cluster analysis and display of genome-wide expression patterns. *Proc Natl Acad Sci USA* **95**, 14863–14868.
[25] Tusher VG, Tibshirani R, and Chu G (2001). Significance analysis of microarrays applied to the ionizing radiation response. *Proc Natl Acad Sci USA* **98**, 5116–5121.
[26] Boyle EI, Weng S, Gollub J, Jin H, Botstein D, Cherry JM, and Sherlock G (2004). GO::TermFinder-open source software for accessing Gene Ontology information and finding significantly enriched Gene Ontology terms associated with a list of genes. *Bioinformatics* **20**, 3710–3715.
[27] van de Vijver MJ, He YD, van't Veer LJ, Dai H, Hart AA, Voskuil DW, Schreiber GJ, Peterse JL, Roberts C, Marton MJ, et al. (2002). A gene-expression signature as a predictor of survival in breast cancer [see comment]. *New Engl J Med* **347**, 1999–2009.
[28] Sorlie T, Tibshirani R, Parker J, Hastie T, Marron JS, Nobel A, Deng S, Johnsen H, Pesich R, Geisler S, et al. (2003). Repeated observation of breast tumor subtypes in independent gene expression data sets. *Proc Natl Acad Sci USA* **100**, 8418–8423.
[29] R Development Core Team (2005). *R: A language and environment for statistical computing, reference index version 2.2.1*. R Foundation for Statistical Computing, Vienna, Austria. ISBN 3-900051-07-0. Availbale at http://www.R-project.org.
[30] Wascher RA, Huynh KT, Giuliano AE, Hansen NM, Singer FR, Elashoff D, and Hoon DS (2003). Stanniocalcin-1: a novel molecular blood and bone marrow marker for human breast cancer. *Clin Cancer Res* **9**, 1427–1435.
[31] Gerritsen ME, Soriano R, Yang S, Ingle G, Zlot C, Toy K, Winer J, Draksharapu A, Peale F, Wu TD, et al. (2002). *In silico* data filtering to identify new angiogenesis targets from a large *in vitro* gene profiling data set. *Physiol Genomics* **10**, 13–20.
[32] Lauring J, Abukhdeir AM, Konishi H, Garay JP, Gustin JP, Wang Q, Arceci RJ, Matsui W, and Park BH (2008). The multiple myeloma associated *MMSET* gene contributes to cellular adhesion, clonogenic growth, and tumorigenicity. *Blood* **111**, 856–864.
[33] Ge H, Si Y, and Roeder RG (1998). Isolation of cDNAs encoding novel transcription coactivators p52 and p75 reveals an alternate regulatory mechanism of transcriptional activation. *EMBO J* **17**, 6723–6729.
[34] Mukherjee DP, McTiernan CF, and Sen S (1993). Myotrophin induces early response genes and enhances cardiac gene expression. *Hypertension* **21**, 142–148.
[35] Al-Hajj M, Wicha MS, Benito-Hernandez A, Morrison SJ, and Clarke MF (2003). Prospective identification of tumorigenic breast cancer cells. *Proc Natl Acad Sci USA* **100**, 3983–3988.
[36] Ferrara N, Hillan KJ, Gerber HP, and Novotny W (2004). Discovery and development of bevacizumab, an anti-VEGF antibody for treating cancer. *Nat Rev Drug Discov* **3**, 391–400.
[37] Sorlie T, Perou CM, Tibshirani R, Aas T, Geisler S, Johnsen H, Hastie T, Eisen MB, van de Rijn M, Jeffrey S, et al. (2001). Gene expression patterns of breast carcinomas distinguish tumor subclasses with clinical implications. *Proc Natl Acad Sci USA* **98**, 10869–10874.
[38] van't Veer LJ, Dai H, van de Vijver MJ, He YD, Hart AA, Mao M, Peterse HL, van der Kooy K, Marton MJ, Witteveen AT, et al. (2002). Gene expression profiling predicts clinical outcome of breast cancer. *Nature* **415**, 530–536.
[39] Chang HY, Nuyten DS, Sneddon JB, Hastie T, Tibshirani R, Sorlie T, Dai H, He YD, van't Veer LJ, Bartelink H, et al. (2005). Robustness, scalability, and integration of a wound-response gene expression signature in predicting breast cancer survival. *Proc Natl Acad Sci USA* **102**, 3738–3743.
[40] Liu R, Wang X, Chen GY, Dalerba P, Gurney A, Hoey T, Sherlock G, Lewicki J, Shedden K, and Clarke MF (2007). The prognostic role of a gene signature from tumorigenic breast-cancer cells. *N Engl J Med* **356**, 217–226.
[41] Reya T, Morrison SJ, Clarke MF, and Weissman IL (2001). Stem cells, cancer, and cancer stem cells. *Nature* **414**, 105–111.
[42] Fillmore CM and Kuperwasser C (2008). Human breast cancer cell lines contain stem-like cells that self-renew, give rise to phenotypically diverse progeny and survive chemotherapy. *Breast Cancer Res* **10**, R25.
[43] Kok M, Koornstra RH, Margarido TC, Fles R, Armstrong NJ, Linn SC, Van't Veer LJ, and Weigelt B (2009). Mammosphere-derived gene set predicts outcome in patients with ER-positive breast cancer. *J Pathol* **8**, 316–326.
[44] Honeth G, Bendahl PO, Ringner M, Saal LH, Gruvberger-Saal SK, Lovgren K, Grabau D, Ferno M, Borg A, and Hegardt C (2008). The $CD44^+/CD24^-$ phenotype is enriched in basal-like breast tumors. *Breast Cancer Res* **10**, R53.
[45] Charafe-Jauffret E, Ginestier C, Iovino F, Wicinski J, Cervera N, Finetti P, Hur MH, Diebel ME, Monville F, Dutcher J, et al. (2009). Breast cancer cell lines contain functional cancer stem cells with metastatic capacity and a distinct molecular signature. *Cancer Res* **69**, 1302–1313.
[46] Kaplan RN, Riba RD, Zacharoulis S, Bramley AH, Vincent L, Costa C, MacDonald DD, Jin DK, Shido K, Kerns SA, et al. (2005). VEGFR1-positive haematopoietic bone marrow progenitors initiate the pre-metastatic niche. *Nature* **438**, 820–827.
[47] Calabrese C, Poppleton H, Kocak M, Hogg TL, Fuller C, Hamner B, Oh EY, Gaber MW, Finklestein D, Allen M, et al. (2007). A perivascular niche for brain tumor stem cells. *Cancer Cell* **11**, 69–82.
[48] Chi JT, Chang HY, Haraldsen G, Jahnsen FL, Troyanskaya OG, Chang DS, Wang Z, Rockson SG, van de Rijn M, Botstein D, et al. (2003). Endothelial cell diversity revealed by global expression profiling. *Proc Natl Acad Sci USA* **100**, 10623–10628.
[49] Chang HY, Sneddon JB, Alizadeh AA, Sood R, West RB, Montgomery K, Chi JT, van de Rijn M, Botstein D, and Brown PO (2004). Gene expression signature of fibroblast serum response predicts human cancer progression: similarities between tumors and wounds. *PLoS Biol* **2**, E7.
[50] Bogaerts J, Cardoso F, Buyse M, Braga S, Loi S, Harrison JA, Bines J, Mook S, Decker N, Ravdin P, et al. (2006). Gene signature evaluation as a prognostic tool: challenges in the design of the MINDACT trial. *Nat Clin Pract Oncol* **3**, 540–551.